Preparation of sponge-like porous SiO$_2$ antireflective coatings with excellent environment-resistance by an acid-catalysed sol–gel method

Bibo Xia,[a] Jianhui Luo,[bc] Yuanyang Li,[a] Bowen Yang,[a] Shuming Zhang[a] and Bo jiang [iD] *[a]

Silica coatings with high-transmittance and good environment-resistance properties were prepared by an acid-catalyzed sol–gel method without template. Hexamethyldisilazane (HMDS) was added into an acid-catalyzed silica sol which acted not only as the catalyst but also as a blocking agent. The effect of different contents of HMDS has been investigated. The sponge-like silica coating was obtained when the weight ratio of HMDS to SiO$_2$ was higher than 90%. The addition of HMDS enabled these silica antireflective coatings to possess excellent hydrophobicity properties. When the weight ratio of HMDS to SiO$_2$ was 100%, the silica coating exhibited transmittance as high as 99.64% at a given wavelength and static water contact angle of 143.0°. After 48 hours of environment aging testing at 40%, 60% and 80% RH, these coatings showed a minute decrease upon maximum transmittance, from 99.64% to 99.56%, 99.49% and 99.38%, respectively. The sponge-like HMDS-containing coatings exhibited easy-to-clean properties, which would have great potential application in laser systems.

1. Introduction

Antireflective (AR) coatings have been widely used in optical devices such as solar cells, laser systems and cathode ray tubes.[1–3] The reflective index of coating (n_c) and actual thickness of coating (d_c) are decisive factors for obtaining an ideal homogeneous AR coating which achieves effectively 100% transmittance at a specific wavelength, that is, n_c is equal to $(n_a n_s)^{0.5}$, where n_a and n_s are the refractive indices of the air and the substrate, respectively; and d_c should be $\lambda/4n_c$, where λ is the wavelength of incident light.[4,5] A typical glass has a refractive index between 1.45 and 1.65 in the visible spectral region, which implies that the refractive index of a matched AR coating must be between 1.20 and 1.25. For instance, BK-7 ($n = 1.52$) requires a refractive index as low as 1.23. Dielectric materials such as silica, alumina, and titania with refractive indices of 1.45, 1.65, and 2.3, respectively, were widely used as AR coatings. The refractive index can be lowered by introducing nanopores ($n = 1$) into AR coatings.[6] Several methods have been applied to generate nanoporous AR coatings, including etching,[7,8] oblique-angle deposition,[9,10] reactive twin-magnetron sputtering,[11] phase separation and self-assembly of block copolymers,[12] the

layer-by-layer deposition method,[13] and the sol–gel process.[14] Compared with other methods, sol–gel-derived AR coating has many advantages, such as low cost, simple operation process and controllable structure.[15]

Sol–gel acid-catalyzed silica coatings, possessing remarkable abrasion-resistance, have attracted tremendous attention in both academic and industrial areas.[16–18] The growth of silica gel with acid catalyzed sol–gel process results in a structure of linear chains which leads to a strong adhesive force on the substrate and a high refractive index about 1.42.[19] Therefore, an ideal AR coating cannot be obtained by just depositing single pure acid-catalyzed film on typical glass. Generation of micro pore in the silica film by porogen, which can be post-removed, is an efficient method to create micropore. Low molecular weight compound,[20] surfactant[16,21] and polymer[22,23] acting as porogen had been studied widely. Nonetheless, high calcination temperature is undesirable for certain polymer substrate during the removal of additional porogen.

Here we report a new approach to generate manopore in the acid-catalyzed silica film so as to prepare low refractive index acid-catalyzed silica coating without porogen. When added into the acid-catalyzed silica sol, on the one hand, HMDS releases ammonia which can act as catalyzer; on the other hand, the volume effect of tri-methylsilyl group can hinder the conden-sation reaction. The importance of these two effects depends on the content of HMDS in the acid sol. Addition of HMDS changes deeply the morphology of the resulting acid-catalyzed silica film, by transforming the chain-silica to sponge-like porous silica. As the tri-methylsilyl group in the HMDS can afford the

[a]Key Laboratory of Green Chemistry & Technology, College of Chemistry, Sichuan University, Chengdu 610064, China. E-mail: jiangbo@scu.edu.cn

[b]Research Institute of Petroleum Exploration & Development (RIPED), PetroChina, China

[c]Key Laboratory of Nano Chemistry (KLNC), CNPC, P.O.Box 910, 20# Xueyuan Road, Haidian District, Beijing 100083, P. R. China

film good hydrophobicity,[24,25] by adjusting the content of HMDS, sponge-like porous coatings with high-transmittance and prominent environmental resistance properties can be obtained.

2. Experimental section

2.1. Materials

Tetraethylorthoxylsilicane (TEOS, $Si(OC_2H_5)_4$, 98%) and hexamethyldisilazane (HMDS, $(CH_3)_3SiNHSi(CH_3)_3$, 98%) were purchased from Acros and Alfa Aesar. Ethyl alcohol (C_2H_5OH, 99.7%) and concentrated hydrochloric acid (HCl, 37%) were purchased from Kelong Chemical Reagents Factory (Chengdu City, Sichuan Province, China). Ethyl alcohol was distilled twice before use. The water was deionized. All chemicals were used without further purification.

2.2. Preparations of sponge-like porous coatings

The sol–gel HMDS-containing acid-catalyzed coatings were fabricated as follows: a solution of tetraethylorthoxylsilicane, ethyl alcohol, H_2O and HCl was first prepared and stirred for 2 hours at 30 °C. The molar ratio of TEOS : H_2O : C_2H_5OH : HCl was $1 : 4.01 : 36.83 : 4.16 \times 10^{-3}$ and the final concentration of SiO_2 was 3% by weight. The sol was aged in a water-bathing at 25 °C for 7 days and then refluxed for 24 hours to remove the catalyst (HCl), filtered through a 0.22 μm polyvinylidene fluoride (PVDF) filter. The resultant sol (named acid-catalyzed silica sol) was stored at room temperature for use. Hexamethyldisilazane was mixed in acid-catalyzed silica sol with the weight ratio of HMDS to SiO_2 ($W_{H/S}$) varying from 0% to 200%, and then stirred for 2 hours at 30 °C, the prepared sol was diluted twice prior to use. The borosilicate glass substrates (BK-7) were cleaned by ultrasonication in acetone for 10 min, and then wiped carefully with cleanroom wipers. Afterwards the silica sols were deposited on substrates by dip-coating at the withdrawal rate of 30 mm min^{-1} at 40 Relative Humidity (RH). The coatings were treated at 160 °C for 2 hours.

2.3. Characterization

To determine particle size and distribution, the silica sols were analyzed by dynamic light scattering (DLS, Malvern Nano-ZS, wavelength of 632.8 nm) at 25 °C. The transmission spectra were measured with a UV-vis spectrophotometer (Mapada, UV-3200PC), with wavelength ranging from 300–1100 nm. Before transmission spectra measurement, the film thicknesses of AR coatings were optimized by varying the withdrawal rate and sol concentration. The structures of the HMDS-containing colloids were investigated with a transmission electron microscope (JEOL, JEM-100CX) operated at 200 kV. The samples were prepared on a holey carbon coated copper grid by placing a drop of the colloidal suspension used for coatings. SEM (JSM-5900LV) was used to observe the surface profile and cross section structure of coatings at low vacuum conditions. Static water contact angles of the coatings were performed using a contact angle meter (Krüss DSA100 Germany). To investigate the environment aging resistance of silica coatings, the prepared coatings were put into an unventilated cabin for 48 hours, whose humidity were 40%, 60% and 80% RH and temperature was 25 °C. Ammonia hardening experiment: HMDS-containing acid-catalyzed coatings were put into an unventilated cabin saturated with ammonia for 12 hours at 60 °C.

3. Results and discussion

Particle size and its distribution were investigated by DLS and are shown in Fig. 1. For an AR coating prepared from silica sol, the sol particle structure is important factor which affect the values of the refractive index of the AR coating. The condensation reaction of TEOS under acid catalyzed conditions is an electrophilic reaction, as a result, chain-structured silica were formed.[26] The particle size of pure acid-catalyzed silica sol is under 5 nm.[26] When HMDS was added and the $W_{H/S}$ was lower than 90%, gelation occurred during the aging process of the HMDS-containing acid-catalyzed silica sol. The number particle size of different content of HMDS-modified acid-catalyzed silica sol was shown in Fig. 1. The average diameter of particle was 18.5 nm, when $W_{H/S}$ was 100%. While the $W_{H/S}$ increased to 150% and 200%, the corresponding particle size was 10.1 nm and 8.1 nm. It is indicated that a bigger size of silica particle was formed on account of the addition of HMDS.

When added into an acid-catalyzed silica sol, HMDS reacted with chain-structured silica by substituting hydroxyl group with tri-methylsilyl group and released ammonia as catalyst. Under ammonia conditions, intermolecular hydroxyl group or intramolecular hydroxyl groups aggregated with each other through condensation reaction. Silica chains gathered together and formed the net silica structure. Meanwhile HMDS played another role on supplying the tri-methylsilyl which took the place of exterior hydroxyl group, hence hindered the condensation. Addition of HMDS resulted two competition effects, the release ammonia catalyst accelerated the condensation reaction
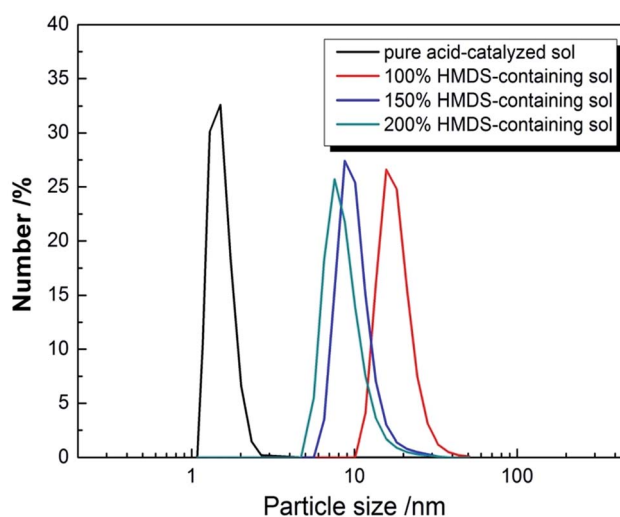

Fig. 1 Particle size number of pure, 100%, 150% and 200% HMDS-containing acid-catalyzed silica sols.

of chain-structured acid-catalyzed silica, and tri-methylsilyl group prevented the silica structures from further condensation reaction. When the content of HMDS was small, there were not enough tri-methylsilyl to substitute with exterior hydroxyl group to counterbalance the effect of ammonia catalyst, the silica sol would polymerize excessively and gelation of the sol occurred during aging. When the $W_{H/S}$ was too high, the redundant tri-methylsilyl would substitute the most hydroxyl group, the polymerization of the silica sol would decrease dramatically, and then there would not be enough silica with certain size and shape. Only when the content of HMDS was appropriate, the effects of catalyst ammonia and tri-methylsilyl's hindering counterbalanced and silica nanoparticle with diameter ranging from 10 nm to 20 nm were obtained. It explains the particle size decreased as the $W_{H/S}$ increased from 100% to 200%. The TEM of 100% HMDS-containing acid-catalyzed silica coatings are shown in Fig. 2(a). The HMDS-modified acid-catalyzed silica agglomerated easily and turned into floccules structure. However, it is easily found that network structure generated by chain-structured silica appeared at the edge of TEM image. After deposited on silica wafer, the surface profile SEM and cross section SEM of 100% HMDS-containing acid-catalyzed silica coatings were depicted in Fig. 2(b) and (c). It is obvious that the 100% HMDS-containing acid-catalyzed coating showed as porous structure with uneven nanopore size. As the shape of HMDS-containing silica nanoparticle was irregular and the nanoparticle size was not uniform, after randomly stacking on substrate, the nanopore size of HMDS-containing coatings was also uneven. This porous structure with uneven nanopore size was called "sponge-like structure".

Owing to the discrepancy of refractive indices between air and optical substrate (BK-7, $n = 1.52$), the transmittance of optical substrate in visible spectral region is about 91.8%. So, it is necessary to deposit coatings with corresponding refractive index on optical element to enhance the transmittance. Pure acid-catalyzed silica coating, which is composed of chain-structured silica, possesses a refractive index as high as 1.42. By depositing one-layer acid-catalyzed silica coating on BK-7 merely, it only brings an improvement of 3.5% upon transmittance as shown in Fig. 3. The addition of HMDS changed the morphology of acid-catalyzed silica, and decreased the refractive index of
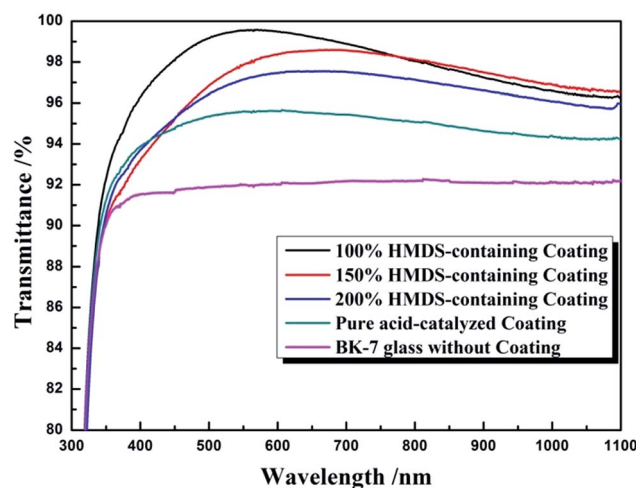

Fig. 3 Spectral transmittance of borosilicate glass, acid-catalyzed coating and HMDS-containing coatings.

coating, hence increased transmittance of resulted coating. When the $W_{H/S}$ was 100%, HMDS-containing silica coating achieved a transmittance as high as 99.64%, bringing a significant improvement upon transmittance. When the $W_{H/S}$ increased to 150% or 200%, the transmittance of HMDS-containing silica coatings were 98.82% or 97.56%, probably due to a higher packing of a smaller silica particles during gel process.

Kim et al. suggested that the hydrophobic nature of a silica thin film was closely linked to the AR durability of the AR coating.[27] Hydrophobicity can be monitored by the water contact angle (WCA). As shown in Fig. 4, pure acid-catalyzed silica coating was hydrophilic with a WCA of 60.5°. Because of the addition of HMDS, the WCA of containing silica coating enhanced conspicuously. When the $W_{H/S}$ was 100%, 150% and 200%, the coating's WCA reached to 143.0°, 145° and 148°, respectively. The environmental resistance properties of pure and HMDS-modified acid-catalyzed silica coating were investigated by putting them in saturated containers with 40%, 60% and 80% RH for 48 hours at 25 °C. We measured the maximum transmittance of as-prepared coatings and processed coatings. The change in maximum transmittance as a function of relative humidity after testing for 48 hours was shown in Fig. 4. It was
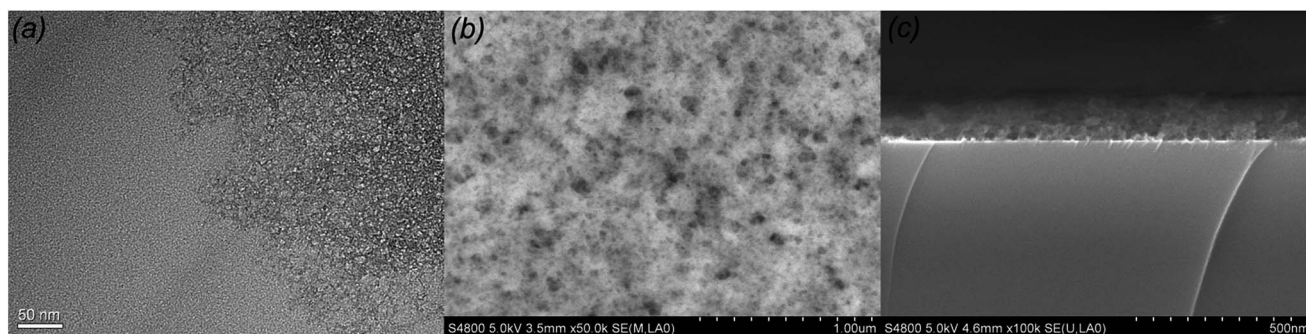

Fig. 2 TEM of 100% HMDS-containing acid-catalyzed coating (a), surface SEM of 100% HMDS-containing acid-catalyzed coating (b) and cross section SEM of 100% HMDS-containing acid-catalyzed coating (c).
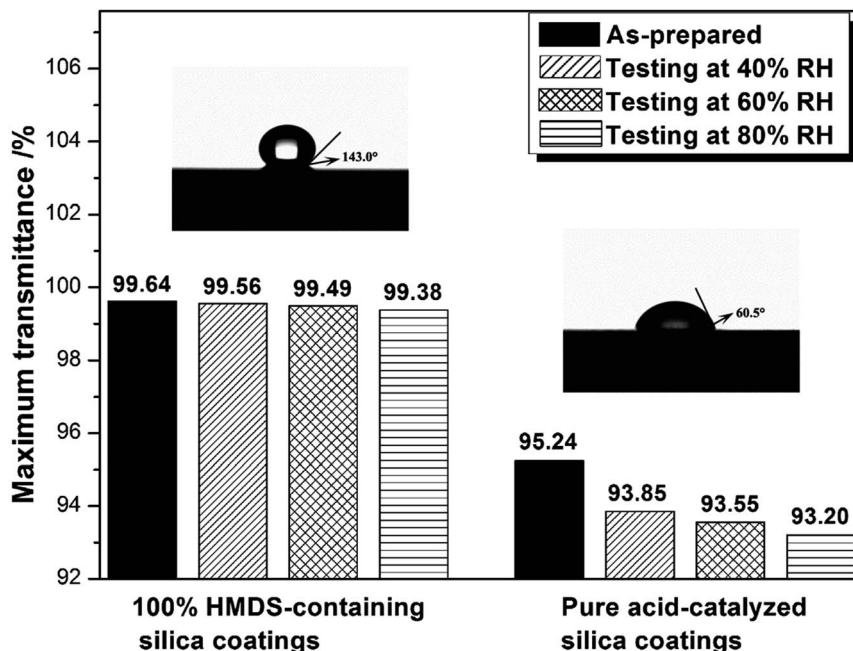
Fig. 4 Static water contact angle of pure acid-catalyzed coating and 100% HMDS-containing acid-catalyzed coating; change in maximum transmittance as a function of relative humidity after testing for 48 hours at 25 °C.

found that after testing for 48 hours the pure acid-catalysed silica coating showed striking decrease on maximum transmittance, from 95.24% to 93.85%, 93.55% and 93.20% for 40%, 60% and 80% RH, respectively. However, 100%-HMDS acid-catalysed silica coatings only showed minute decrease upon maximum transmittance, from 99.64% to 99.56%, 99.49% and 99.38%, respectively. So these HMDS-modified acid-catalysed silica coatings could be considered to possess excellent environment aging resistance properties.

The growth of silica gel with acid catalyzed sol–gel process results in a structure of linear chains which leads to a strong adhesive force on the substrate and good abrasion resistance, however, the random assembly of sponge-like nanoparticle endowed the HMDS-containing coatings with poor mechanical durability, in other words, the easy-to-clean properties. A lot of works have been reported to address the mechanical durability of nanoparticle silica coatings,[28,29] inspired by that, the ammonia hardening experiment had been applied to enhance the mechanical durability of the HMDS-containing acid-catalyzed coatings. Unfortunately, after ammonia modification, the HMDS-containing coating didn't show significant improvement on abrasion resistance properties. So, it was concluded that there almost remained no residual hydroxyl group in 100% HMDS-containing acid-catalyzed coating. These antireflective coatings with excellent environment aging resistance properties and easy-to-clean properties would have greatly potential application in laser systems.[30]

4. Conclusion

Antireflective silica coatings with environment resistance properties and easy-to-clean performance derived from acid-catalyzed silica were prepared *via* sol–gel process. We presented a new method to decrease the refractive index of acid-catalyzed silica coating by changing the morphology of chain-structured silica. The addition of HMDS into acid-catalyzed silica sol not only accelerated the polymerization but also introduced excellent hydrophobicity properties. These coatings with excellent performance may have a wide range of application in optical systems.

Acknowledgements

Notes and references

1 B. G. Prevo, E. W. Hon and O. D. Velev, *J. Mater. Chem.*, 2007, **17**, 791–799.

2 L. Zhang, Z. Qiao, M. Zheng, Q. Huo and J. Sun, *J. Mater. Chem.*, 2010, **20**, 6125–6130.

3 P. Prené, J. J. Priotton, L. Beaurain and P. Belleville, *J. Sol-Gel Sci. Technol.*, 2000, **19**, 533–537.

4 B. G. Prevo, Y. Hwang and O. D. Velev, *Chem. Mater.*, 2005, **17**, 3642–3651.

5 W. T. Wang, N. Lu, J. Y. Hao, H. B. Xu, D. P. Qi and L. F. Chi, *J. Phys. Chem. C*, 2010, **114**, 1989–1995.

6 H. Hattori, *Adv. Mater.*, 2001, **12**, 51–54.

7 B. Dudem, J. W. Leem and J. S. Yu, *RSC Adv.*, 2016, **6**, 3764–3773.

8 M. Ibn-Elhaj and M. Schadt, *Nature*, 2001, **410**, 796–799.

9 J. Q. Xi, M. F. Schubert, J. K. Kim, E. F. Schubert, M. Chen, S. Y. Lin, W. Liu and J. A. Smart, *Nat. Photonics*, 2007, **1**, 176–179.

10 J. Q. Xi, J. K. Kim and E. F. Schubert, *Nano Lett.*, 2005, **5**, 1385–1387.

11 J. Szczyrbowski, G. Bräeuer, M. Ruske, G. Teschner and A. Zmelty, *J. Non-Cryst. Solids*, 1997, **218**, 262–266.

12 X. Li, L. Xue and Y. Han, *J. Mater. Chem.*, 2011, **21**, 5817–5827.

13 J. Hiller, J. D. Mendelsohn and M. F. Rubner, *Nat. Mater.*, 2002, **1**, 59–63.

14 Y. Du, L. E. Luna, W. S. Tan, M. F. Rubner and R. E. Cohen, *ACS Nano*, 2010, **4**, 4308–4316.

15 D. R. Uhlmann, T. Suratwala, K. Davidson, J. M. Boulton and G. Teowee, *J. Non-Cryst. Solids*, 1997, **218**, 113–122.

16 L. Yao and J. He, *J. Mater. Chem. A*, 2014, **2**, 6994.

17 H. Ye, X. Zhang, Y. Zhang, L. Ye, B. Xiao, H. Lv and B. Jiang, *Sol. Energy Mater. Sol. Cells*, 2011, **95**, 2347–2351.

18 H. K. Raut, A. S. Nair, S. S. Dinachali, V. A. Ganesh, T. M. Walsh and S. Ramakrishna, *Sol. Energy Mater. Sol. Cells*, 2013, **111**, 9–15.

19 G. Wu, J. Wang, J. Shen, T. Yang, Q. Zhang, B. Zhou, Z. Deng, B. Fan, D. Zhou and F. Zhang, *Mater. Sci. Eng., B*, 2000, **78**, 135–139.

20 D. Zhao, Q. Huo, J. Feng, B. F. Chmelka and G. D. Stucky, *J. Am. Chem. Soc.*, 1998, **120**, 6024–6036.

21 L. Ye, S. Zhang, Q. Wang, L. Yan, H. Lv and B. Jiang, *RSC Adv.*, 2014, **4**, 35818–35822.

22 B. Xia, Q. Zhang, S. Yao, Y. Zhang, B. Xiao and B. Jiang, *J. Sol-Gel Sci. Technol.*, 2014, **71**, 291–296.

23 Y. Li, H. Lv, L. Ye, L. Yan, Y. Zhang, B. Xia, H. Yan and B. Jiang, *RSC Adv.*, 2015, **5**, 20365–20370.

24 M. Manca, A. Cannavale, L. D. Marco, A. S. Aricò, R. Cingolani and G. Gigli, *Langmuir*, 2009, **25**, 6357–6362.

25 X. X. Zhang, S. Cai, D. You, L. H. Yan, H. B. Lv, X. D. Yuan and B. Jiang, *Adv. Funct. Mater.*, 2013, **23**, 4361–4365.

26 A. Vincent, S. Babu, E. Brinley, A. Karakoti, S. Deshpande and S. Seal, *J. Phys. Chem. C*, 2007, **111**, 8291–8298.

27 S. Kim, J. Cho and K. Char, *Langmuir*, 2007, **23**, 6737–6743.

28 P. F. Belleville and H. G. Floch, *Proc. SPIE*, 1994, **2288**, 25–32.

29 I. S. Bayer, *Coatings*, 2017, **7**, 12.

30 D. Glöß, P. Frach, C. Gottfried, S. Klinkenberg, J.-S. Liebig, W. Hentsch, H. Liepack and M. Krug, *Thin Solid Films*, 2008, **516**, 4487–4489.